Turkish Journal of Chemistry
http://journals.tubitak.gov.tr/chem/
Research Article

Turk J Chem
(2015) 39: 159 – 168

doi:10.3906/kim-1407-49

Preparation of visible light sensitive nano-sized N-TiO_2 photocatalysts and their photocatalytic activity under visible light

Young-Gu KANG, Kwang-Hyeok LEE, Hyun-Sik HAHM*
Department of Chemical Engineering, Myongji University, Cheoin-gu, Yongin, Gyeonggi-do, Korea

Received: 25.07.2014 • **Accepted:** 12.10.2014 • **Published Online:** 23.01.2015 • **Printed:** 20.02.2015

Abstract: This study aimed to develop a photocatalyst that responds to visible light. For the preparation of visible light sensitive photocatalysts, N was doped into TiO_2 (N-TiO_2). To inhibit the recombination of excited electrons and holes, transition metals (M = Pt, Cu, Fe, Cr) were loaded on the N-TiO_2. N-TiO_2 nanotubes were also synthesized by a hydrothermal treatment of the prepared N-TiO_2 in a strong basic environment. The prepared photocatalysts were characterized by XRD, FESEM, HRTEM, XPS, and UV/VIS spectrophotometer, and their photocatalytic activity was tested by the photodecomposition of liquid-phase methylene blue and gas-phase acetone.

Key words: Visible light sensitive TiO_2, N-doping, transition metal loading, N-TiO_2 nanotubes

1. Introduction

TiO_2 is a photocatalyst well known for its photostability, inertness, compatibility, strong oxidizing power, and affordable price.[1–3] However, while a major portion of the sunlight that reaches the Earth is visible light (about 50%), TiO_2 responds only to UV light, which comprises a mere 4% of sunlight. In this context, it is necessary to make TiO_2 respond to visible light.[4]

Through the modification of TiO_2 band gap, it is possible to make TiO_2 respond to visible light (red shift). Nitrogen doping is one of the modification methods to lower the TiO_2 band gap.[5–11] Hiroshi prepared TiO_2-N_x that responds to visible light by annealing TiO_2 in the ammonia gas environment and proved 20% photodecomposition efficiency of isopropyl alcohol in visible light.[12] However, it is also known that the N-doping increases the possibility of the recombination of excited electrons and holes.[13,14] Thus, to increase the photocatalytic activity of a photocatalyst, it is necessary to reduce the recombination of excited electrons and holes. One of the possibilities to do this is transition metal loading.

By loading a transition metal on TiO_2, the Fermi level of the transition metal locates in the middle of the valence and conduction bands of TiO_2. In this case, if the Fermi level of the transition metal locates under the conduction band of TiO_2, the electrons excited from the valence band of the TiO_2 move to the transition metal.[13] Through this effect, the recombination of excited electrons and holes is inhibited.[11]

Another method to improve photocatalytic activity is to increase the surface area of a photocatalyst.[15,16] Various nanostructured materials, such as nanotubes, nanorods, and nanofibers, are now widely synthesized for this purpose. TiO_2 nanotubes have been synthesized by the template-assisted method,[17,18] electrochemical anodic oxidation method,[19,20] and sol-gel method.[21,22] However, these methods have some disadvantages,

*Correspondence: hahm@mju.ac.kr

namely, impurity inclusion by templates, complexity of the preparation process, and high cost, respectively. In 1998, Kasuga et al. synthesized TiO_2 nanotubes by a simple and inexpensive hydrothermal method.[23]

In the present study, we focused on the development of nano-sized TiO_2 photocatalysts that respond to visible light. In order to respond to visible light, N-doping was employed. To increase the efficiency of photocatalysts, the recombination of excited electrons and holes must be inhibited. For this purpose, transition metals (Pt, Cu, Fe, Cr) were loaded on N-doped TiO_2. N-TiO_2 nanotubes were also synthesized by the hydrothermal method. The photocatalytic activity of the prepared photocatalysts was tested by the photodecomposition of liquid-phase methylene blue and gas-phase acetone.

2. Results and discussion

2.1. Effect of pH on the phase, particle size, and photocatalytic activity of N-TiO_2 nanopowders

In the preparation of TiO_2 nanopowders by the sol-gel method, pH can affect the morphology, size, and photocatalytic activity.[24] In order to examine the effect of pH, it was maintained at 2.0, 4.7, and 9.0 in the catalysts' preparation.

XRD results of the prepared N-TiO_2 nanopowders are presented in Figure 1. The XRD patterns show that the prepared N-TiO_2 nanopowders have anatase phase regardless of pH and that N-TiO_2 nanopowders prepared at pH 9 show the highest crystallinity. The particle sizes of the prepared N-TiO_2 nanopowders were calculated by using Scherrer equation[24] with FWHM (full width at half maximum) taken at 2 $\theta = 25^\circ$. The calculated particle sizes were 5.42 nm, 5.99 nm, and 7.58 nm at pH 2.0, 4.7, and 9.0, respectively, showing that the particle size increases with pH. This result coincides with the report that, in the sol-gel synthesis, the addition of an acid suppresses the hydrolysis reaction and leads to a smaller particle and the addition of a base facilitates the hydrolysis reaction and leads to a larger particle.[25]

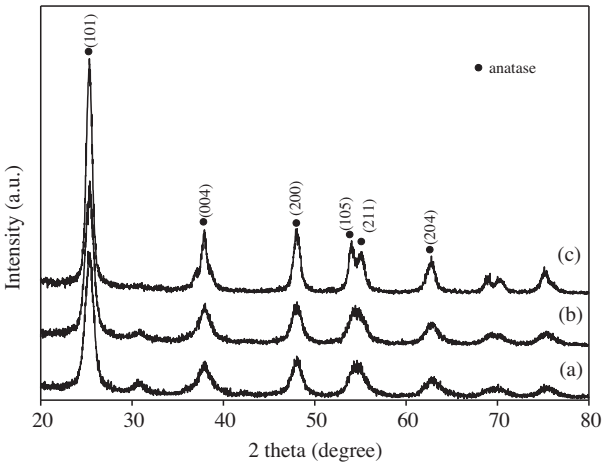

Figure 1. XRD patterns of N-TiO_2 nanopowders prepared at (a) pH 2.0, (b) pH 4.7, and (c) pH 9.0.

In order to test the photocatalytic activity of the prepared N-TiO_2 nanopowders, 50 mL of methylene blue aqueous solution (300 ppm) was photo-decomposed under visible light (4 fluorescent lamps) with 0.2 g of the prepared N-TiO_2 nanopowders, and the result is presented in Figure 2. As shown, N-TiO_2 nanopowders prepared at pH 2.0 and 4.7 showed no photocatalytic activity under visible light, whereas N-TiO_2 nanopowder prepared at pH 9.0 showed about 43% methylene blue decomposition in 4 h. This result may be due to the degree of crystallinity of the prepared N-TiO_2 nanopowders. The N-TiO_2 nanopowders prepared at pH 9.0

showed the highest crystallinity. Consequently, the catalysts used at the later part of this study were prepared at pH 9.0.

2.2. Transition metal (M) loading on N-TiO_2 nanopowders and its photocatalytic activity

In order to improve photocatalytic efficiency, the recombination of excited electrons and holes should be inhibited. To do so, transition metals were loaded on the prepared N-TiO_2 nanopowders. The Fermi level of the transition metals locates between the valence band and conduction band of TiO_2. In this case, the electrons excited from the valence band to the conduction band could easily move to the transition metal, inhibiting the recombination.[13] Transition metals [Cr (4.5 eV), Fe (4.7 eV), Cu (4.65 eV), Pt (5.65 eV)] whose work functions are larger than that of TiO_2 (4.2 eV) were chosen for this study.[26]

The photocatalytic activity of transition metal-loaded N-TiO_2 (M-N-TiO_2) reduced by hydrogen was examined by the decomposition of methylene blue aqueous solution (50 mL, 300 ppm) under visible light (4 fluorescent lamps) with 0.2 g of prepared M-N-TiO_2 photocatalysts, and the results are presented in Figure 3. As shown, there was no remarkable catalytic activity observed under visible light.

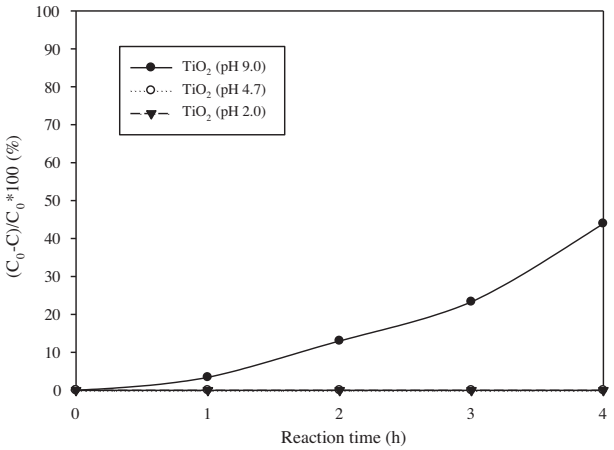

Figure 2. Photocatalytic decomposition of methylene blue (300 ppm, 50 mL) under 40-W fluorescent lamps with 0.2 g of N-TiO_2 nanopowders prepared at different pH.

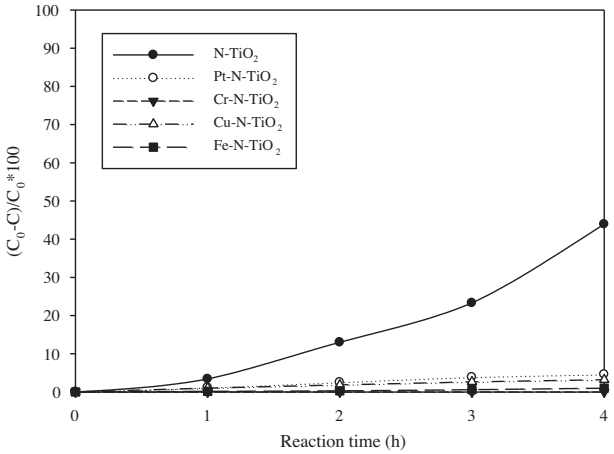

Figure 3. Photocatalytic decomposition of methylene blue (300 ppm, 50 mL) under 40-W fluorescent lamps with 0.2 g of M-N-TiO_2 (M = Pt, Cr, Cu, Fe) catalysts reduced by H_2 at 400 °C for 3 h.

The photocatalytic activity of M-N-TiO_2 catalysts reduced by $NaBH_4$ was also examined by the decomposition of methylene blue, and the results are presented in Figure 4. As shown, Pt-N-TiO_2 and Cu-N-TiO_2 catalysts showed high photocatalytic decomposition efficiencies of 92% and 75%, respectively. These results show that the photocatalytic activity of M-N-TiO_2 catalysts largely depends on the reduction method and reducing power of the reducing agents. The order of photocatalytic activity of M-N-TiO_2 catalysts was Pt > Cu >> Fe ≈ Cr. This result might stem from the fact that Pt has the highest work function compared to other transition metals used. The work function of Pt is higher than the level of the conduction band of TiO_2, and so the excited electrons can easily move to Pt, inhibiting the recombination of excited electrons and holes. Although Cu, Fe, and Cr have similar work functions, the electric resistance of Cu (16.78 nΩ∘ m) is lower than those of Fe (96 nΩ∘ m) and Cr (125 nΩ∘ m); consequently, the catalyst loaded with Cu might show a higher activity than those loaded with Fe and Cr. From the results above, we know that the catalysts reduced by $NaBH_4$ show a higher photocatalytic activity.

For the gas-phase experiment, 0.2 g of M-N-TiO_2 photocatalysts reduced by $NaBH_4$ was coated on the inner surface of a quartz tube (its volume was 60 mL) and 8.71×10^{-4} mol of acetone was introduced into the tube. Then, under visible light, a photocatalytic decomposition reaction was carried out and the results are presented in Figure 5. As shown, Pt-N-TiO_2 showed the highest photocatalytic decomposition efficiency (about 50%) as in the case of the liquid-phase methylene blue decomposition. The order of photocatalytic activity of M-N-TiO_2 catalysts was Pt > Cu > Fe $\approx$ Cr. This result was similar to the result of liquid-phase methylene blue decomposition as well. From this result, we learn that the transition metal-loaded photocatalysts (M-N-TiO_2) show a high photocatalytic activity in the gas-phase under visible light as well.

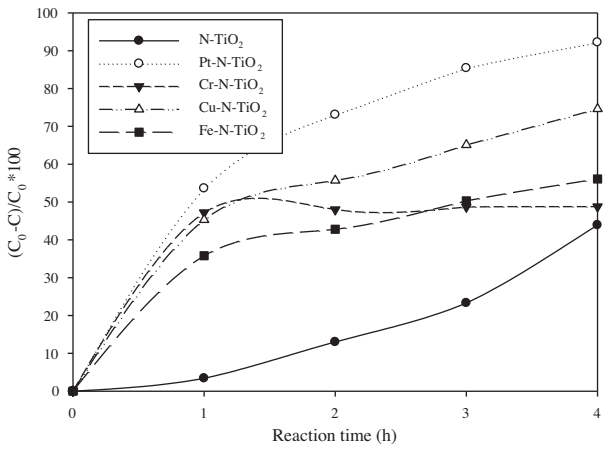

Figure 4. Photocatalytic decomposition of methylene blue (300 ppm, 50 mL) under 40-W fluorescent lamps with 0.2 g of M-N-TiO_2 (M = Pt, Cr, Cu, Fe) catalysts reduced by $NaBH_4$.

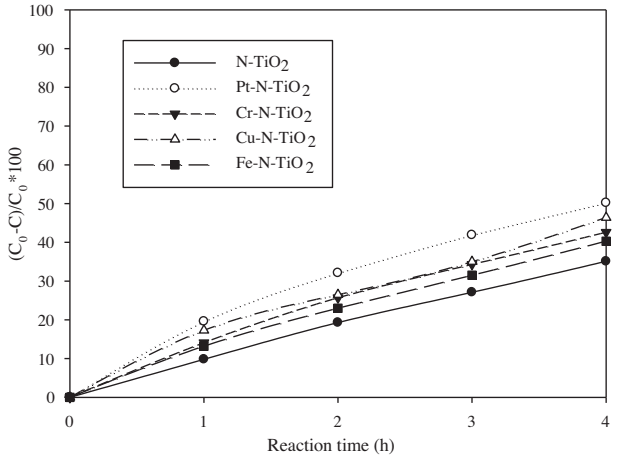

Figure 5. Photocatalytic decomposition of acetone gas (8.71×10^{-4} mol) under 40-W fluorescent lamps with 0.2 g of M-N-TiO_2 (M=Pt, Cr, Cu, and Fe) catalysts reduced by $NaBH_4$.

As mentioned above, the photocatalysts reduced by $NaBH_4$ showed a higher photocatalytic activity. Therefore, XPS analysis was carried out with Cu-N-TiO_2 reduced by the two methods, and the results are presented in Figure 6. XPS peaks at 952.5 eV and 932.5 $\sim$ 932.8 eV correspond to Cu $2p_{1/2}$ and $2p_{3/2}$ of Cu^0, respectively.[3] Comparing these spectra in Figure 6a and Figure 6b, it was established that the catalyst reduced by $NaBH_4$ showed higher peak intensity, that is, $NaBH_4$ showed a better reduction ability than H_2. We usually use hydrogen to reduce materials, but the results shown if Figures 3 and 4 provide an important insight that the selection of reduction reagents is very important and affects the photocatalytic activity.

Although N-doping gives rise to the red shift, it also provides sites for the recombination of excited electrons and holes, reducing thus the photocatalytic activity.[5–10] However, as mentioned above, transition metal-loaded N-TiO_2 photocatalysts reduced by $NaBH_4$ showed a high photocatalytic activity under visible light. This result suggests that the transition metals loaded on N-TiO_2 inhibit the recombination of excited electrons and holes, increasing the photocatalytic activity, and that the reduction method of the transition metal precursors is also important.

2.3. Synthesis of N-TiO_2 nanotubes (N-TNT) and their photocatalytic activity

Another way to improve photocatalytic efficiency of a photocatalyst is to increase its surface area. To do so, N-TiO_2 nanotubes (N-TNT) were synthesized by hydrothermal treatment of the prepared N-TiO_2 nanopowders.

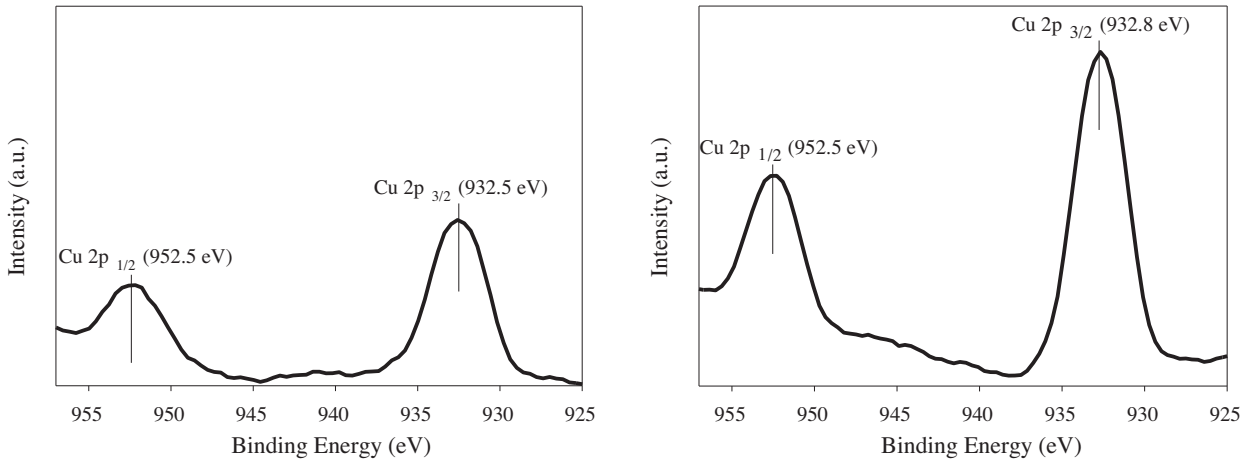

Figure 6. XPS spectra of Cu-N-TiO_2 catalysts reduced by (a) H_2 and (b) $NaBH_4$.

During the synthesis of N-TiO_2 nanotubes, the structure change of the material was checked by FE-SEM with time, and the results are presented in Figure 7. As shown in the FE-SEM images, the starting material (N-TiO_2

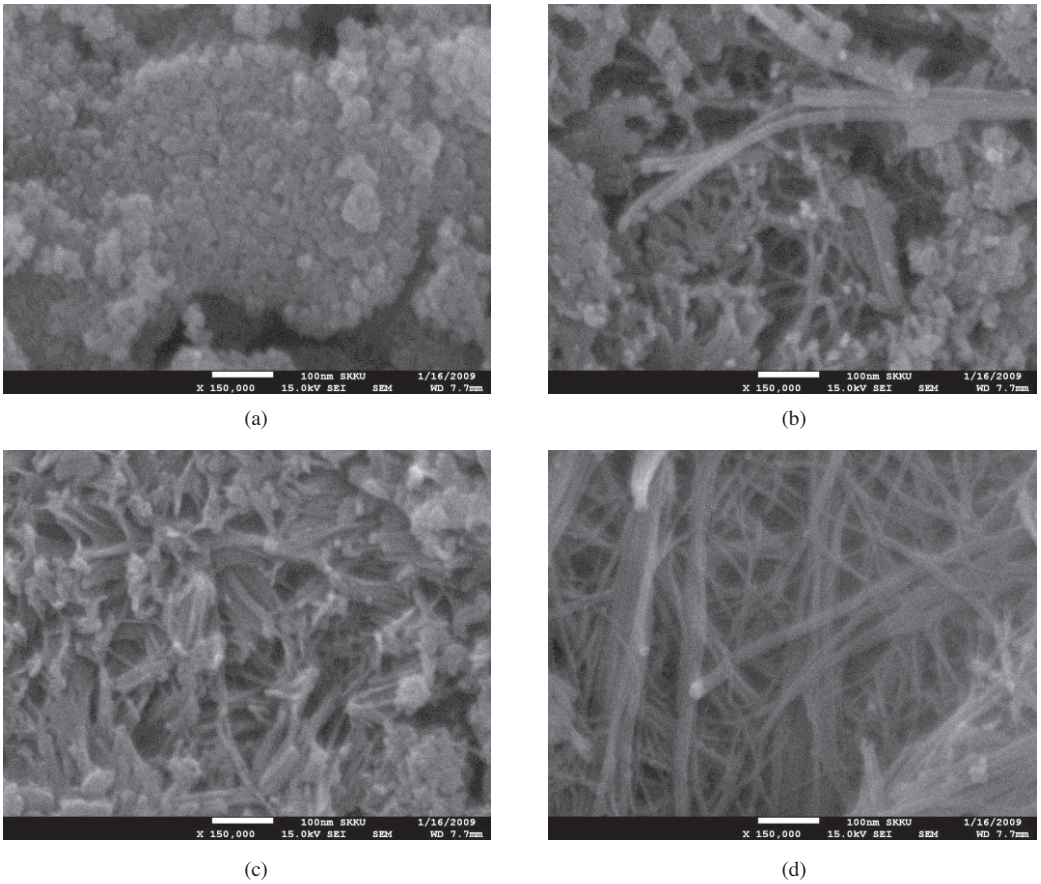

Figure 7. FE-SEM images of the products produced by a hydrothermal treatment of N-TiO_2 nanopowder with 10 M NaOH at 120 °C for (a) 0 h, (b) 6 h, (c) 12 h, and (d) 24 h.

nanopowders) consists of relatively uniform-sized powders (Figure 7a). It was also found that the nanotubes started to grow from the nanopowders (Figure 7a) and, as time went by, the length of the nanotubes increased (Figures 7b–7d). After 24 h, N-TiO_2 nanotubes of the 7 $\sim$ 17 nm diameter and the length of several thousand nm were observed (Figure 7d). From this result, we can infer that, in the 10 M NaOH strong basic environment, OH^- ions cleave TiO_2 nanopowders and produce Ti-O and that Na^+ ions connect the cleaved Ti-O such as Ti-O^--Na^+-O^--Ti, producing N-TiO_2 nanotubes.[27] This result coincides with the report by Dimitry that the length of a N-TiO_2 nanotube is proportional to the amount of TiO_2 powder used.[16]

TEM and HRTEM images of the synthesized N-TiO_2 nanotubes are presented in Figure 8. As shown, well-structured N-TiO_2 nanotubes thousands of nanometers in length were observed (Figure 8a), while the diameters of the synthesized N-TiO_2 nanotubes were observed to be 7 $\sim$ 17 nm (Figure 8b).

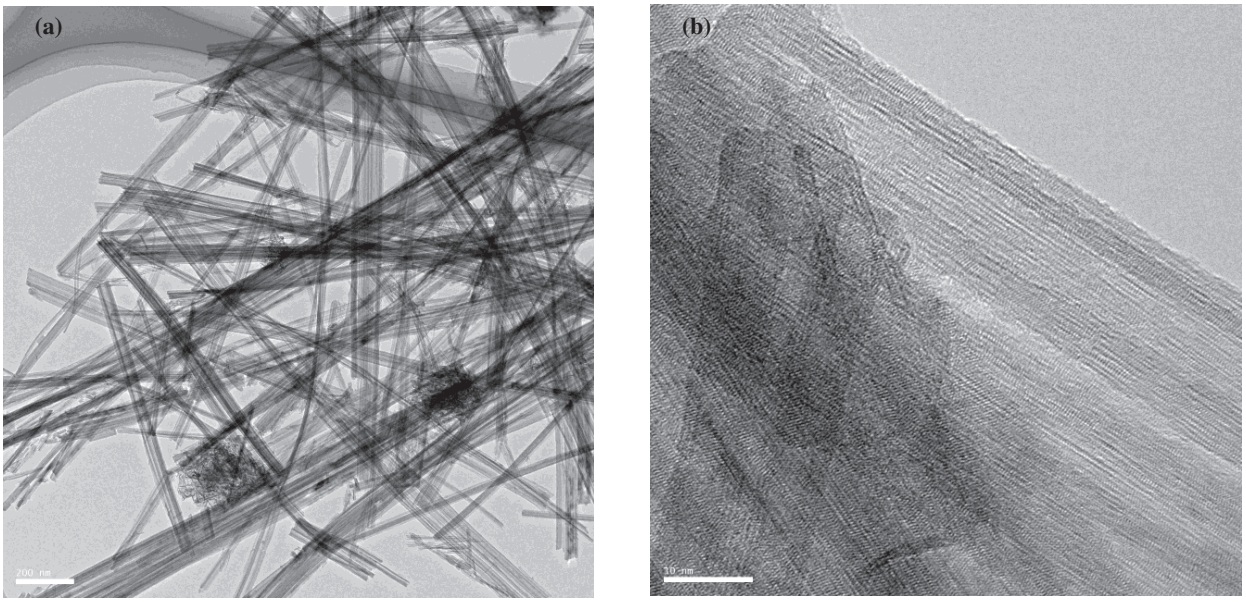

Figure 8. TEM (a) and HRTEM (b) images of synthesized N-TiO_2 nanotubes calcined at 400 °C for 1 h.

In order to check the structure of the synthesized N-TiO_2 nanotubes, XRD analysis was carried out. Figure 9 shows the XRD patterns of (a) N-TiO_2 nanopowder starting material; (b) titanate nanotube washed with 0.1 M HCl solution and distilled water; and (c) titanate nanotube calcined at 400 °C for 1 h. There were some differences in the spectra (see Figures 9a and 9b): a characteristic peak of titanate nanotube was found around 2 $\theta = 10^\circ$ in the spectrum of Figure 9b; moreover, the anatase TiO_2 main peak at 2 $\theta = 25^\circ$ disappeared and two new characteristic peaks of titanate nanotube were observed at 2 $\theta = 23^\circ$ and 28° in the spectrum of Figure 9b. Chen also reported these peaks (2 $\theta = 23^\circ$ and 28°) and stated that the peaks were relevant to the protonic titanate nanotube.[28] The spectrum of Figure 9c, corresponding to a N-TiO_2 nanotube calcined at 400 °C for 1 h, shows that while the peaks around 2 $\theta = 10^\circ$, 23°, and 28° disappear, the main peak of anatase TiO_2 at 2 $\theta = 25^\circ$ reappears. As shown in Figures 8 and 9, the nanotube structure did not break by the calcination at 400 °C for 1 h. From these results, it was also established that by calcination the protonic titanate nanotube at 400 °C turned to a N-TiO_2 nanotube and the washing and calcining of the products produced by the hydrothermal treatment of N-TiO_2 nanopowders were very important steps to produce an active N-TiO_2 nanotube photocatalyst.

2.4. Decomposition of methylene blue by M-N-TNT

There have been many attempts to treat dye-wastewater by some mesoporous materials, such as activated carbons, MCM-22, and MCM-41.[29,30] However, while these materials have an adsorbing ability, they cannot decompose the pollutants. In this sense, M-N-TNT has the abilities of both adsorption and decomposition, and so the adsorption and decomposition abilities of the synthesized M-N-TNT were tested by the adsorption and decomposition of methylene blue aqueous solutions.

In general, TNT (TiO_2 nanotube) produced by the hydrothermal method has a band gap of 3.87 eV, which means that UV light ($\sim$ 320 nm) is needed to activate the TNT.[5] In order to see whether the M-N-TNT responds to visible light (380 $\sim$ 800 nm), UV-VIS absorbance of M-N-TNT was measured (see the results in Figure 10). As shown in Figure 10, M-N-TNT produced by the loading of transition metals on N-TNT responded to visible light (red shift), implying that the M-N-TNT could be used as a photocatalyst under visible light.

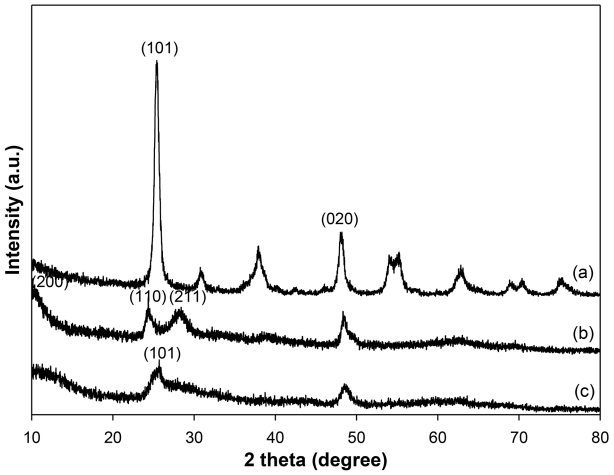

Figure 9. XRD patterns of (a) N-TiO_2, (b) titanate nanotube washed with 0.1 M HCl and distilled water, and (c) N-TiO_2 nanotube calcined at 400 °C for 1 h.

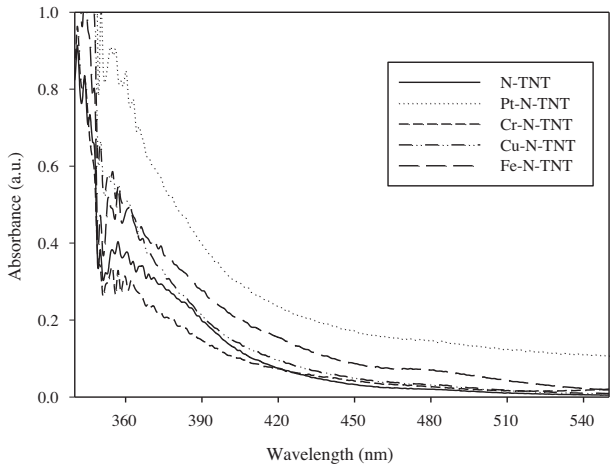

Figure 10. UV/VIS spectra of M-N-TNT reduced by $NaBH_4$.

The adsorption and photodecomposition ability of M-N-TNT photocatalysts was tested with 50 mL of methylene blue aqueous solution (500 ppm) under visible light (4 fluorescent lamps) with 0.1 g of the synthesized M-N-TNT photocatalysts (see the results in Figure 11). After the adsorption equilibrium (at 0" h) was reached, four fluorescent lamps were turned on and the photodecomposition of methylene blue took place under visible light. In Figure 11, the first steep rise of the curves (from 0 to 0' h) corresponds to the adsorption of methylene blue into M-N-TNT photocatalysts; the section from 0' to 0" h corresponds to the adsorption equilibrium step; afterwards, a slow rise in the curves corresponds to the photodecomposition of methylene blue under visible light. The order of the amount of the adsorption was Pt-N-TNT $\approx$ N-TNT $>$ Fe-N-TNT $\approx$ Cu-N-TNT $>$ Cr-N-TNT. Among the M-N-TNT photocatalysts used, Pt-N-TNT and Cu-N-TNT showed a high photodecomposition ability. In the case of Pt-N-TNT photocatalyst, the adsorption and photocatalytic decomposition efficiency was about 98%. These results show that M-N-TNT photocatalysts can be used to treat dye-wastewaters.

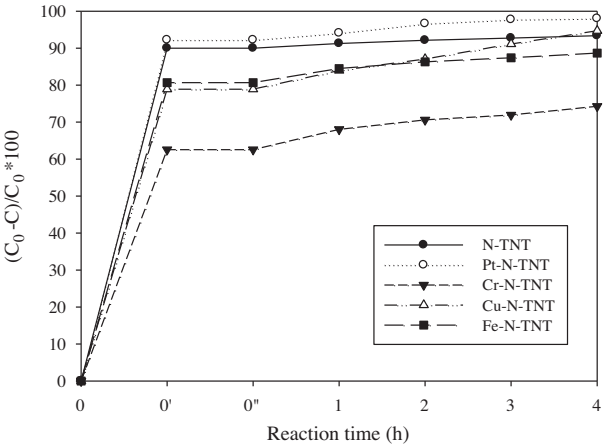

Figure 11. Adsorption and photocatalytic decomposition of methylene blue (500 ppm and 50 mL) under 40-W fluorescent lamps with 0.1 g of M-N-TNT reduced by $NaBH_4$.

3. Experimental

3.1. Materials

For the preparation of TiO_2 photocatalysts, titanium butoxide ($Ti(OC_4H_9)_4$, Aldrich) was used as a precursor, ethanol (Duksan) as a cosolvent for mixing of titanium butoxide, and water. For N-doping, NH_4OH solution (25%, Dae Jung) was used. To synthesize a TiO_2 nanotube from the prepared TiO_2 powder, sodium hydroxide (Duksan) was used. For the transition metal loading, H_2PtCl_6 (SIGMA), $Cr(NO_3)_3 \cdot 9H_2O$ (SAMCHUN), $Cu(NO_3)_3 \cdot 3H_2O$ (Junsei), and $Fe(NO_3)_3 \cdot 9H_2O$ (SAMCHUN) were used.

3.2. Preparation of N-doped TiO_2 (N-TiO_2) nanopowder

N-TiO_2 nanopowder was prepared by the sol-gel method using titanium butoxide as a precursor.[31] In the preparation, the molar ratio of water to titanium butoxide was 150:1 and the molar ratio of cosolvent ethanol to titanium butoxide was 50:1. The mixture was stirred at 70 °C for 30 min. Then, for N-doping, NH_4OH was added to the solution until the pH of the solution became 9; then the solution was stirred at room temperature for 6 h. After the preparation, the mixture was dried at 80 °C for 12 h, finely ground in a mortar, and then calcined at 550 °C for 3 h under air environment.

3.3. Preparation of the N-TiO_2 nanotube

The N-TiO_2 nanotube was synthesized by the hydrothermal method using the prepared N-TiO_2 nanopowder as a starting material.[32,33] First, 2 g of the N-TiO_2 nanopowder was mixed with 150 mL of 10 M NaOH; then the mixed solution was placed in an autoclave (120 °C) for different times of 6, 12, and 24 h. The product was separated by centrifugation, washed with 0.1 N HCl solution three times, and washed with distilled water three times. Afterwards, to obtain the N-TiO_2 nanotube, the product was dried at 80 °C for 24 h and calcined at 400 °C for 1 h under air environment.

3.4. Transition metal (M) loading

Transition metals (Pt, Cr, Fe, Cu) were loaded on the prepared N-TiO_2 nanopowder by the impregnation method. The pre-calculated amount of a transition metal compound (0.053 g H_2PtCl_6, 0.16 g $Cr(NO_3)_3 \cdot 9H_2O$,

0.196 g $Fe(NO_3)_3 \cdot 9H_2O$, 0.182 g $Cu(NO_3)_3 \cdot 3H_2O$) was dissolved in 50 mL of distilled water and 2 g of N-TiO_2 nanopowder was added to the solution; then the mixture was held at room temperature for 3 h. The impregnated N-TiO_2 was separated from the mixture by centrifugation, dried at 80 °C for 15 h, and then calcined at 400 °C for 1 h under air environment. The calcined catalysts were reduced at 400 °C for 3 h under hydrogen environment. Another reduction method was as follows: the abovementioned transition metal-impregnated N-TiO_2 that was separated from the mixture by centrifugation was reduced with 300 mL of 0.125 M $NaBH_4$ solution for 3 h and then separated from the solution by centrifugation; afterwards, it washed with distilled water 3 times and, finally, dried at 80 °C for 15 h.

Transition metals (Pt, Cr, Fe, Cu) were also loaded on the N-TiO_2 nanotube by the impregnation method and reduced by $NaBH_4$ as mentioned above.

3.5. Characterization of photocatalysts

The structure and particle size of the prepared TiO_2 photocatalysts were characterized by XRD (Cu K_α radiation, PANalytical X'pert-Pro); their morphology was examined by field emission scanning electron microscopy (FESEM, JSM7500F). The structure of the synthesized N-TiO_2 nanotube was observed by a high resolution transmission electron microscopy (HRTEM, JEM2100). To establish the oxidation state of the transition metals, XPS (X-ray photoelectron spectrophotometer, ESCA 2000) analysis was also performed. The UV/VIS absorbance of the prepared photocatalysts was measured by a UV/VIS spectrophotometer (Varian, Cary-5000).

3.6. Activity test of the prepared photocatalysts

The photocatalytic activity of the prepared catalysts was tested by the decomposition of methylene blue (liquid-phase) and acetone (gas-phase) under visible light. As a visible light source, four 10-W fluorescent lamps were used. The spectrum of the fluorescent lamp is presented in Figure 12.

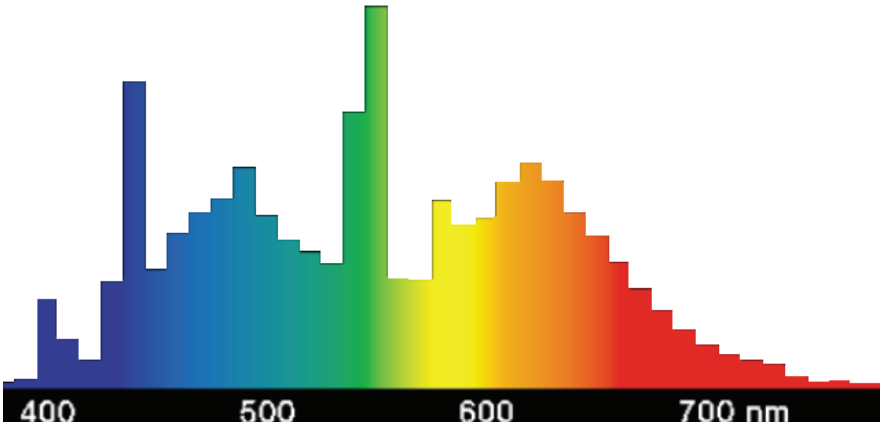

Figure 12. Spectrum of fluorescent lamps.

For the liquid phase photocatalytic activity test, 0.2 g of the prepared photocatalyst was suspended in 50 mL of 300 ppm methylene blue solution. The concentration change of methylene blue under visible light was measured with a UV-VIS spectrophotometer with an interval of 1 h. The wavelength of 655 nm was selected for the analysis of methylene blue.

For the gas phase photocatalytic activity test, 0.1 g of the prepared photocatalyst was coated on the inner surface of a Pyrex tube (60 mL). Then 0.064 mL of acetone was injected into the tube. The injected acetone was vaporized and decomposed under visible light and measured with GC with an interval of 1 h.

The efficiency of photocatalytic decomposition was defined as follows:

$$\text{Photocatalytic decomposition efficiency (\%)} = ((\text{Co} - \text{C})/\text{Co}) \times 100,$$

where Co = initial concentration of methylene blue; C = concentration of the remaining methylene blue.

Acknowledgment

This work was supported by 2013 Research Fund of Myongji University.

References

1. Chae, Y. K.; Park, J. W.; Mori, S.; Suzuki, M. *Korean J. Chem. Eng.* **2013**, *30*, 62–66.
2. Zendehzaban, M.; Sharifnia, S.; Hosseini, S. N. *Korean J. Chem. Eng.* **2013**, *30*, 574–579.
3. Fujishima, A.; Rao, T. N.; Tryk, D. A. *J. Photochem. Photobiol. C* **2000**, *1*, 1–21.
4. Wantala, K.; Khemthong, P.; Wittayakun, J.; Grisdanurak, N. *Korean J. Chem. Eng.* **2011**, *28*, 2178–2183.
5. Valentin, C. D.; Finazzi, E.; Pacchioni, G.; Selloni, A.; Livraghi, S.; Paganini, M. C.; Giamello, E. *Chem. Phys.* **2007**, *339*, 44–46.
6. Asahi, R.; Morikawa, T.; Ohwaki, T.; Aoki, K.; Taga, Y. *Science* **2001**, *293*, 269–271.
7. Wang, Y.; Feng, C.; Jin, Z.; Zhang, J.; Yang, J.; Zhang, S. *J. Mol. Catal. A: Chem.* **2006**, *260*, 1–3.
8. Zhang, J.; Wang, Y.; Jin, Z.; Wu, Z.; Zhang, Z. *Appl. Surf. Sci.* **2008**, *254*, 462–466.
9. Xu, J. H.; Li, J.; Dai, W. L.; Cao, Y.; Li, H.; Fan, K. *Appl. Catal., B* **2008**, *79*, 72–80.
10. Huang, L.; Sun, Z.; Liu, Y. *J. Ceram. Soc. Jpn.* **2007**, *115*, 28–31.
11. Morikawa, T.; Ohwaki, T.; Suzuki, K. I.; Moribe, S.; Shozo, T. K *Appl. Catal., B* **2008**, *83*, 56–62.
12. Hiroshi, I.; Yuka, W.; Kazuhito, H. *J. Phys. Chem. B* **2003**, *107*, 5483–5486.
13. Meng, N.; Michael, K. H.; Leung, Y. C.; Sumathy, K. *Renewable Sustainable Energy Rev.* **2007**, *11*, 401–425.
14. Torres, G. R.; Lindgren, T.; Lu, J.; Granqvist, C. G.; Lindquist, S. E. *J. Phys. Chem. B* **2004**, *108*, 5995–6003.
15. Ou, H. H.; Lo, S. L. *Sep. Purif. Technol.* **2007**, *58*, 179–191.
16. Dimitry, V. B.; Jens, M. F.; Frank, C. W. *Adv. Mater.* **2006**, *18*, 2807–2824.
17. Michailowski, A.; Almawlawi, D.; Cheng, G.; Moskovits, M. *Chem. Phys. Lett.* **2001**, *349*, 1–5.
18. Liu, S. M.; Gan, L. M.; Liu, L. H.; Zhang, W. D.; Zeng, H. C. *Chem. Mater.* **2002**, *14*, 1391–1397.
19. Ghicov, A.; Tsuchiya, H.; Macak, J. M.; Schmuki, P. *Electrochem. Commun.* **2005**, *7*, 505–509.
20. Varghese, O. K.; Gong, D.; Paulose, M.; Ong, K. G.; Dickey, E. C.; Grimes, C. A. *Adv. Mater.* **2003**, *15*, 624–627.
21. Lakshmi, B. B.; Patrissi, C. J.; Martin, C. R. *Chem. Mater.* **1997**, *9*, 2544–2550.
22. Jung, S. C. *Korean J. Chem. Eng.* **2008**, *25*, 364–367.
23. Kasuga, T.; Hiramatsu, M.; Hoson, A.; Sekino, T.; Niihara, K. *Langmuir* **1998**, *14*, 3160–3163.
24. Li, B.; Wang, X.; Yan, M.; Li, L. *Mater. Chem. Phys.* **2002**, *78*, 184–188.
25. Carp, O.; Huisman, C. L.; Reller, A. *Prog. Solid State Chem.* **2004**, *32*, 33–177.
26. Kaneko, M.; Okura, I. (Eds.) *Photocatalysis: Science and Technology*; Springer, USA, 2002, pp. 33–36.
27. Wang, S.; Li, H.; Xu, L. *J. Colloid Interface Sci.* **2006**, *295*, 71–78.
28. Ho, K. Y.; McKay, G.; Yeung, K. L. *Langmuir* **2003**, *19*, 3019–3024.